Heavy Ion Physics with Compact Muon Solenoid at LHC

I.P.Lokhtin, L.I.Sarycheva
Institute of Nuclear Physics, Moscow State University,
Vorobievy Gory, 119899 Moscow, Russia
for the CMS Collaboration

Abstract

The Compact Muon Solenoid (CMS) is the general purpose detector designed to run at the LHC and optimized mainly for the search of the Higgs boson in proton-proton collisions. However, a good muon system and electromagnetic and hadron calorimeters with fine granularity gives the possibility to cover several important aspects of the heavy ion physics. In particular, the production of heavy quarkonia Υ, Υ', Υ'' through their muon decay channel and the energy losses of hard quark- and gluon-initiated jets, are valuable processes for studying the phase transition from the hadronic matter to the plasma of deconfined quarks and gluons in central nucleus-nucleus collisions. $Z(\rightarrow \mu^+\mu^-)$ production will be also detected in heavy ion collisions and can be used as reference process for understanding conventional nuclear effects. Transverse energy deposition in barrel, end-cap and very forward parts of the CMS calorimeters are expected to be correlated with decreasing impact parameter of nucleus-nucleus collision, thus giving us a tool to measure the centrality of the collision.

1 Introduction

The experimental study of ultrarelativistic nuclear collisions offers the unique possibility of studying the properties of strongly interacting matter at the high energy density at which it is expected that hadronic matter becomes deconfined and a gas of asymptotically free quarks and gluons is formed, the so-called quark-gluon plasma (QGP), in which the colour interactions between partons is screened owing to collective effects (see, for example, reviews [1]-[5]). A feature which distinguished high energy collisions of heavy nuclei from the corresponding hadron-hadron interactions is the possibility of producing super-dense matter in volumes which are quasi-macroscopic on characteristic hadronic scales. This opens up the possibility in principle of using the thermodynamics of strong interactions.

The significant progress attained recently in the modeling of QCD systems on the lattice, in particular, including dynamical quarks, allows one to state with some certainty that the deconfinement of hadronic matter and chiral symmetry restoration must happen at sufficiently high temperatures $T_c \sim 200$ MeV and (or) baryon-chemical potential [6]. It is assumed that the conditions for realizing the quark-hadron phase transition which, according to the current cosmological ideas, occurred during the first few microseconds of the evolution of the Universe, can be attained as a result of the generation of strongly excited matter in experiments at existing (AGS, SPS) and future (RHIC, LHC) heavy-ion accelerators.

Possible scenarios for production of the QGP in relativistic nucleus-nucleus collisions are still the subject of scientific discussion. In any case, when a significant fraction of the energy of the colliding nuclei is transformed into energy of the constituents of a "thermalized" system, this energy should be sufficient for forming the QGP in a fairly large (compared with typical hadronic scales) volume, when discussion of the theoretical and experimental problems of finding this plasma becomes meaningful. At the present time there is no justification for uniquely interpreting the experimental heavy ion data as signaling the formation of a QGP [7]. The available experimental data on the soft hadron momentum spectra and two-particle correlations indicate on local thermalization of hadronic matter in central collisions of heavy nuclei, a strong longitudinal flow of particles along the collision axis, and, probably, a weak flow in the transverse direction. The observed excess of low-mass dileptons can be interpreted as the result of modification of the masses and decays width of vector mesons in dense matter associated with the partial restoration of chiral symmetry. The enhanced production of strange hadrons is consistent with the assumptions about deconfinement and chiral symmetry restoration, but it can also be described within hadron-cascade models.

In recent years, a great deal of attention has been devoted to the study of "hard" probes of QGP – heavy quarkonia and hard partonic jets, which do not appear as constituents of the thermalized system, but which can carry information about the earliest stages of its evolution. In particular, the strong

suppression of yield of heavy quark vector mesons as J/Ψ, Ψ' ($c\bar{c}$ states) and Υ, Υ', Υ'' ($b\bar{b}$ states) is one of the promising signatures of the quark-gluon plasma formation in heavy ion collisions. It is important to study the mechanisms that governs this effect: the screening $q\bar{q}$ potential by the surrounding colour charges [8], and the dynamical dissociation of bound resonances by semi-hard deconfined gluons [9]. An intriguing phenomenon is the "anomalously" small yield of Ψ-resonances, observed in Pb-Pb collisions in the NA50 experiment (CERN-SPS) [10] and inconsistent with the conventional model of pre-resonance absorption in cold nuclear matter. Although the interpretation of this phenomenon as a result of the formation of a QGP is quite plausible [11], alternative explanations have also been put forward, such, for example, as $\Psi - h$ rescattering on comoving hadrons [12]. Thus the nature of this "anomalous" suppression of Ψ-resonance production is not yet fully understood, and it should be completely explained in future. For heavier ($b\bar{b}$) systems, a similar suppression effect in super-dense strongly interacting matter is expected at higher temperatures than for $c\bar{c}$, which are expected to be reached in central collisions of heavy ions at the RHIC at BNL and LHC at CERN colliders. Here the degrees of suppression of the Υ, Υ' and Υ'' quarkonia, which have different bound-state radii and binding energies, will differ.

Along with the suppression of heavy quarkonia, one of the processes which may give information about the earliest stages of evolution of the dense matter formed in ultrarelativistic nuclear collisions is the passage through the matter of hard jets of colour-charged partons, pairs of which are created at the very beginning of the collision process (typically, at ≤ 0.01 fm/c) as a result of individual initial hard nucleon-nucleon (parton-parton) scatterings. Such jets pass through the dense parton matter formed due to mini-jet production at larger time scales (~ 0.1 fm/c), and interact strongly with the comoving constituents in the medium, changing its original properties as a result of additional rescatterings. The inclusive cross section for hard jet production processes is still very small for performing a systematic analysis of such events at the SPS energies ($\sqrt{s} \simeq 20$ GeV per nucleon), but it increases fast with the energy of colliding nuclei. Therefore these will play important role in the formation of the initial state at the energies of the RHIC ($\sqrt{s} \simeq 200$ GeV per nucleon) and LHC ($\sqrt{s} \simeq 6$ TeV per nucleon) colliders.

The actual problem is to study the energy losses of a hard jet evolving through the dense matter. We know two possible mechanisms of energy losses: (1) radiative losses due to gluon "bremsstrahlung" induced by multiple scattering [13, 14, 15, 16] and (2) collisional losses due to the final state interactions (elastic rescatterings) of high p_T partons off the medium constituents [17, 18]. Since the jet rescattering intensity strongly increases with temperature, formation of a super-dense and hot partonic matter in heavy ion collisions (with initial temperature up to $T \sim 1$ GeV at LHC energies [19]) should result in significantly larger jet energy losses as compared with the case of hadronic gas at $T \leq 0.2$ GeV.

Although the radiative energy losses of a high energy parton have been shown to dominate over the collisional losses by up to an order of magnitude [14], a direct experimental verification of this phenomenon remains an open problem. Indeed, with increasing of hard parton energy the maximum of the angular distribution of bremsstrahlung gluons shifts towards the parent parton direction. This means that measuring the jet energy as a sum of the energies of final hadrons moving inside an angular cone with a given finite size θ_0 will allow the bulk of the gluon radiation to belong to the jet and thus the major fraction of the initial parton energy to be reconstructed. Therefore, the medium-induced radiation will, in the first place, soften particle energy distributions inside the jet, increase the multiplicity of secondary particles, but will not affect the total jet energy. It was recently shown [15] that the radiation of energetic gluons in a QCD medium is essentially different from the Bethe-Heitler independent radiation pattern. Such gluons have formation times exceeding the mean free path for QCD parton scattering in the medium. In these circumstances the coherent effects play a crucial role leading to a strong suppression of the medium-induced gluon radiation. This coherent suppression is a QCD analogue of the Landau-Pomeranchuk-Migdal effect in QED. It is important to notice that the coherent LPM radiation induces a strong dependence of the jet energy on the jet cone size θ_0 [20].

On the other hand, the collisional energy losses represent an incoherent sum over all rescatterings. It is almost independent of the initial parton energy. At the same time, the angular distribution of the collisional energy loss is essentially different from that of the radiative one. The bulk of "thermal" particles knocked out of the dense matter by elastic scatterings fly away in almost transverse direction relative to the hard jet axis. As a result, the collisional energy loss turns out to be practically independent on θ_0 and emerges outside the narrow jet cone. Thus the relative contribution of collisional losses would likely become significant for jets with finite cone size propagating through the QGP [20].

In a search for experimental evidences in favour of the medium-induced energy losses a significant dijet quenching (a suppression of high p_T jet pairs) [21] and a monojet-to-dijet ratio enhancement [22] were proposed as possible signals of dense matter formation in ultrarelativistic collisions of nuclei. Other possible signatures that could directly measure the energy losses involve tagging the hard jet opposite a particle that does not interact strongly as a Z-boson [23] ($q+g \to q+Z \to q+\mu^+ +\mu^-$, $q+\overline{q} \to g+Z \to g+\mu^+ +\mu^-$) or a photon [24] ($q+g \to q+\gamma$, $q+\overline{q} \to g+\gamma$). The advantage of this processes is that one can determine the initial transverse momentum of the hard jet $p_T^{jet} \approx p_T^{\gamma,Z}$. In particular, it gives the challenging possibility to research for coherent effects in QCD-medium: the dependences dE/dx on the initial jet energy or distance traversed can be studied experimentally by varying the energy of the tagged photons (Z-bosons) in the collisions of different nuclei.

The possibility that the high-mass dilepton spectra are modified due to suppression of correlated semileptonic charm and bottom decays, $D\bar{D}$ $(B\bar{B}) \to l^+l^-$, was recently investigated [25] as a sign of large energy losses experienced by c and b quarks.

All the above phenomena (heavy quarkonium yield, dijet and monojet production, $Z+jet$ and $\gamma+jet$ channels, dilepton yield) are important for extracting information about the properties of super-dense matter to be created in ultrarelativistic heavy ion collisions at LHC collider.

2 The Compact Muon Solenoid

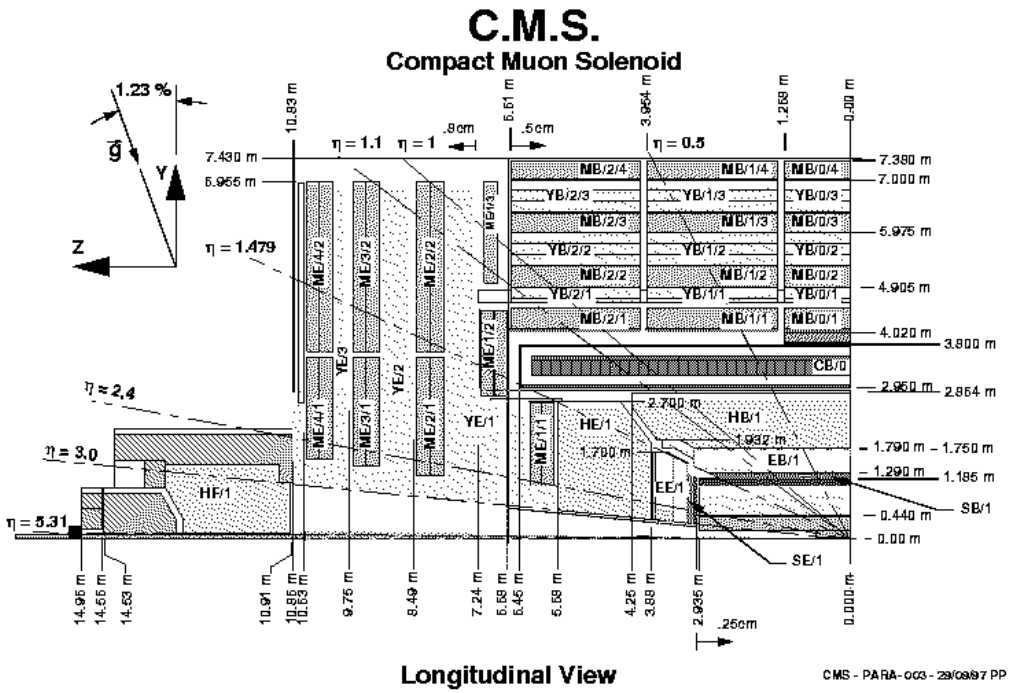

Figure 1: The longitudinal view of CMS detector.

At LHC (Large Hadron Collider) ions will be accelerated up to the energies $E = E_p \times (2Z/A)$ per nucleon pair, where $E_p = 7$ TeV is the proton beam energy for LHC. In the case of Pb nuclei the energy per nucleon pair will be 5.5 TeV and the expected average luminosity for a single experiment is $L \approx 1.0 \times 10^{27}$ cm^{-2}s^{-1}. The interaction cross-section for $Pb-Pb$ collisions is about 8 b, which leads to an event rate of 8 kHz .

The Compact Muon Solenoid (CMS) is the general purpose detector designed to run at the LHC and optimized mainly for the search of the Higgs boson in proton-proton collisions. Accordingly, the detector is optimized for the accurate measurement of the characteristics of high-energy muons, photons, electrons, and hadronic jets, which makes it useful also for studying hard probes of the QGP in heavy ion collisions.

A schematic longitudinal view of the CMS detector is presented in figure 1. The 4π detector consists of a 6 m long and 1.3 m radius central tracker and electromagnetic (ECAL) and hadronic (HCAL) calorimeters located in a strong 4T uniform magnetic field, which is generated by a 13 m long and 6 m diameter solenoid [26]. The electromagnetic calorimeter is made of 80000 $PbWO_4$ crystals, and the hadronic calorimeter consists of scintillator inserted between copper absorber plates. Segmentation in the central "barrel" part of electromagnetic and hadron calorimeters (covering the pseudorapidity region of $\mid \eta \mid < 1.5$) are $\Delta\eta \times \Delta\phi = 0.0145 \times 0.0145$ and $\Delta\eta \times \Delta\phi = 0.087 \times 0.087$ respectively, the expected energy resolution being $\sigma/E(ECAL) = 2\%/\sqrt{E/1\ GeV} \bigoplus 0.5\%$ and $\sigma/E(HCAL) = 70\%/\sqrt{E/1\ GeV} \bigoplus 5\%$. The forward (end-cap) part of the calorimeters covers the pseudo-rapidity region $1.5 \leq |\eta| \leq 3.0$. The CMS calorimetric system also is complemented in the region $3.0 \leq |\eta| \leq 5.0$ by quartz-fiber very forward calorimeters. The CMS muon stations consist of drift tubes in the barrel, cathode strip chambers in the end-caps, and resistive plate chambers.

3 Transverse energy and impact parameter measurements

For studying heavy quarkonium, hard jet and high-mass dimuon production processes in heavy ion collisions, it is extremely important to perform measurements for different centrality of the events (from peripheral to central collisions). The transverse energy deposition in barrel, end-cap and very forward parts of the CMS calorimeters are expected to be correlated with decreasing impact parameter of nucleus-nucleus collision, thus giving us a tool to measure the centrality of the collision and select the most central interaction events with the off-line E_T trigger [27, 28]. The Ca-Ca and Pb-Pb collisions were simulated according to HIJING Monte-Carlo model [29], and the detector response has been modeled using the CMSJET fast simulation program [30]. Figure 2 presents the dependence of the detected transverse energy on the impact parameter for the different parts of the CMS calorimeters. The detected fraction of the initial energy ranges from 86% to 82% for Pb-Pb and from 82% to 76% for Ca-Ca, from central to peripheral collisions respectively.

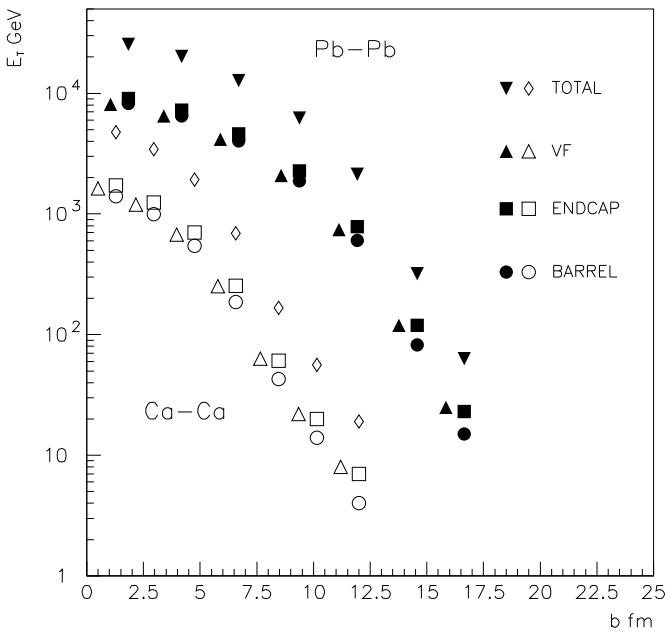

Figure 2: Dependence of the detected transverse energy on the impact parameter of the collisions.

4 Heavy quarkonium production

Detecting Υ-resonance suppression in dense matter is one of the main goals of the physics program of the CMS experiment for heavy ion collisions. CMS detector with its large acceptance muon system $|\eta| < 2.4$ gives unique possibility to study production of the heavy quarkonia via dimuon decay channel. Another important feature of the detector is excellent mass resolution ($\sigma_M \approx 50$ MeV at Υ mass) which makes possible to distinguish different states of Υ family.

To reliably detect and accurately measure the characteristics of Υ resonances, it is necessary to solve the problem of recognizing muon tracks at the strong loads on the tracker detectors expected for central collisions of heavy nuclei. In the case of CMS, the muon momentum can be measured in the central tracker of the detector over a distance of no more than 1.3 m to the interaction vertex. The muons then pass through calorimeters and are recorded in muon chambers. In this case, the muon transverse momentum can be determined with an accuracy of $\leq 1\%$ in a magnetic field of 4 T.

Besides in heavy ion collisions we get the serious problem of the tracker detector occupancy. It may happen in central Pb-Pb collisions (the multiplicity is estimated up to 8000 charged and 4000 neutral particles per rapidity unit) that only these detectors at the distance more than 80 cm, and the pixel detector, would have a reasonable occupancy ($20 - 25\%$). Thus one needs to have an algorithm, which could work effectively and fast under maximum occupancy using only the part of tracker system. The algorithm of dimuon reconstruction in the case of heavy ions with CMS apparatus has been developed recently [31]. The main goal was to find criteria, which would allow getting the maximum number of dimuons from Υ decay as well as providing the maximum suppression of uncorrelated muon pair background from π/K decays, which gives the response in muon stations. The efficiency of reconstruction depends on the multiplicity: in the "central" barrel ($|\eta| < 0.8$) from 66% – for the maximum multiplicity corresponding to central Pb-Pb interactions, up to 90% – for multiplicity reduced by a factor 3. The signal-to-background ratio in Υ mass region is 6 times higher than we have without the algorithm using and almost do not depend on the multiplicity.

In order to estimate the heavy quarkonium rates and signal-to-background ratio [32] in the barrel part of CMS detector covering pseudorapidity region $|\eta| < 0.8$, the Υ-family production cross-section and p_T-distributions were extrapolated from the CDF experimental data [33] at $\sqrt{s} = 1.8$ TeV; the rapidity distributions of resonances were generated according to PYTHIA Monte-Carlo model [34]. The Υ acceptance was calculated by a full simulation of the CMS detector response (program package CMSIM [35]). The resonances were accepted if both decay muons cross any of the muon chambers. An additional cut above the minimum p_T (> 3.5 GeV/c), required to traverse the different materials located before the muon stations in the barrel part of the detector, was applied on each muon. The estimated Υ geometrical acceptance is 16.3% in the whole detector, and 9.5% for the barrel. The dimuon reconstruction efficiency has been also taken into account.

The different background sources are the random decay muons from pions and kaons, and also dimuons from semileptonic open charm and bottom decays ($c\bar{c}(b\bar{b}) \to D\bar{D}$ $(B\bar{B}) \to \mu^+\mu^-$). The scaling of the hard production process cross-section with the size A of the colliding nuclei was taken as $\sigma_{AA} = A^{2\alpha} \times \sigma_{pp}$, where σ_{pp} is the corresponding cross section in pp collisions evaluated using the PYTHIA program [34]. The value α was taken 0.9 for the J/Ψ production, $\alpha = 0.95$ for for the Υ production, and $\alpha = 1.0$ for open charm and bottom production. For a given collision impact parameter the cross-section is assumed to be proportional to the number of binary inelastic nucleon-nucleon sub-collisions, which is determined using a parameterization of the distribution given by the HIJING generator. The background due to the random decay muons from pions and kaons has been generated in the frame of the most pessimistic hypotheses, in particular, with the number of charged particles per rapidity unit to 8000 for a central ($b = 0$) Pb-Pb collisions. The table 1 gives the main contributions to the dimuon mass spectrum in the Υ mass mass interval ($M_\Upsilon \pm 50$ MeV), the rows and the columns indicate the origin of each muon in the pair. The Υ dimuon contribution is, by far, the most dominant, 61.8% of the total; the background is dominated by the π, K decays which contribute to $\approx 65\%$ of the total background with combination of two muons from hadronic decays and with combination with muons from open b or c channels. These pairs of muons are uncorrelated and therefore appear also in the like-sign dimuons mass spectra. Thus the uncorrelated part of the background can be estimated from the $\mu^+\mu^+$ and $\mu^-\mu^-$ events samples by

Table 1: Main contributions (%) to the dimuon mass spectrum in the mass region $M_\Upsilon \pm 50$ MeV/c^2 for Pb-Pb collisions (left) and Ca-Ca collisions (right).

	Υ	π,K	$b\bar{b}$	$c\bar{c}$
Υ	61.8	0.0	0.0	0.0
π,K		13.4	12.8	2.6
$b\bar{b}$			7.2	0.0
$c\bar{c}$				0.0

	Υ	π,K	$b\bar{b}$	$c\bar{c}$
Υ	94.3	0.0	0.0	0.0
π,K		2.7	1.8	0.1
$b\bar{b}$			0.5	0.0
$c\bar{c}$				0.0

Table 2: (Υ/background) ratios and statistics at the Υ mass (left) and at the J/ψ mass (right).

Υ	Pb	Ca
Υ/background	1.6	9.4
N_Υ/month	22000	340000
$N_{\Upsilon'}$/month	7500	115000

J/ψ	Pb	Ca
ψ/background	1.0	9.7
$N_{J/\psi}$/month	10600	220000
$N_{\Psi'}$/month	350	5800

the simple formula:

$$\frac{dN^{back}_{\mu+\mu-}}{dM} = 2\sqrt{\frac{dN_{\mu+\mu+}}{dM}\frac{dN_{\mu-\mu-}}{dM}} \quad (1)$$

and subtracted form the total $\mu^+\mu^-$ distribution. The pure open $c\bar{c}$ contribution is negligible, but not the $b\bar{b}$ contribution.

The mass spectra in the mass range from 8.5 to 11 GeV/c^2 for 1 month of Pb beams with half of the time devoted for data taking (1.3×10^6 s) at the luminosity of $L = 10^{27}$ cm^{-2}s^{-1} are shown in figure 3 for the opposite-sign dimuons. The Υ-states are clearly seen and separated with a signal-to-background ratio equal to 1.6 for the $1S$ resonance. The same mass distribution for Ca-Ca minimum bias collisions is plotted in figure 4. The hadronic background is one order of magnitude lower than in Pb-Pb collisions, the open bottom decays provide the dominant contribution to the background in this case. The signal-to-background ratio amounts to 9.4. The expected signal-to-background ratio together with the available statistics for one month are summarized in table 2. The statistics of 22000 Υ and 7500 Υ' reconstructed resonances for Pb-Pb collisions and 340000 Υ and 115000 Υ' reconstructed resonances for Ca-Ca collisions is high enough to study its yield in different bins of impact parameter.

The J/Ψ production has been studied by the same way, using the same reconstruction efficiencies and the same p_T cuts. The results are shown in table 2 (right). Despite the very low acceptance in the barrel and due to the high production cross-section, the number of J/Ψ in one month is very satisfactory. The opposite-sign dimuon mass spectra for Pb-Pb and Ca-Ca collisions in one month are plotted in figure 5. The J/Ψ resonance is well above the background with a ratio signal-to-background ~ 1 in the case of minimum bias Pb-Pb collisions and ~ 10 for Ca-Ca interactions. In principle, the measured with CMS J/Ψ yield as a function of impact parameter can also provide us the additional information about hot and dense matter created in heavy ion collisions at LHC. However, the Ψ' is not appearing in the spectra being hardly penalized by its cross section.

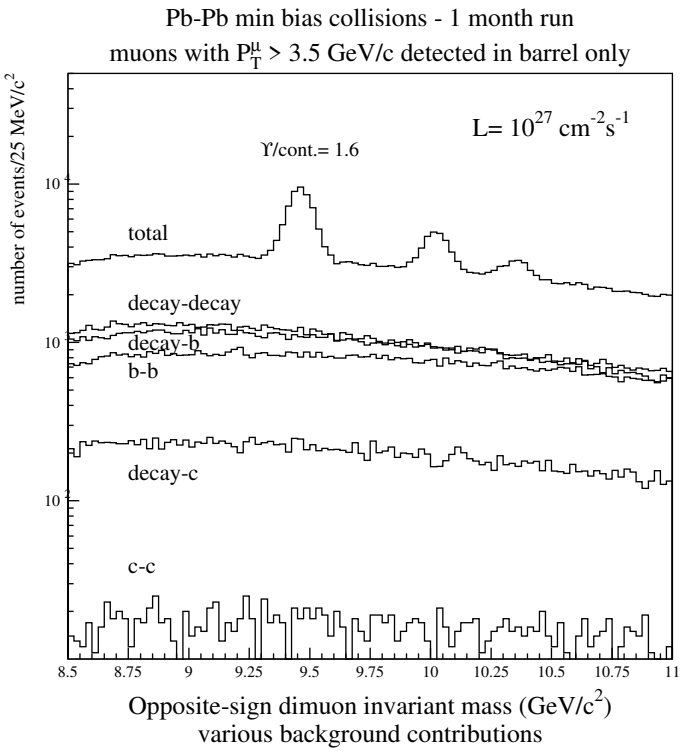

Figure 3: Opposite-sign dimuon mass spectra in the ϒ mass range for Pb-Pb collisions in one month.

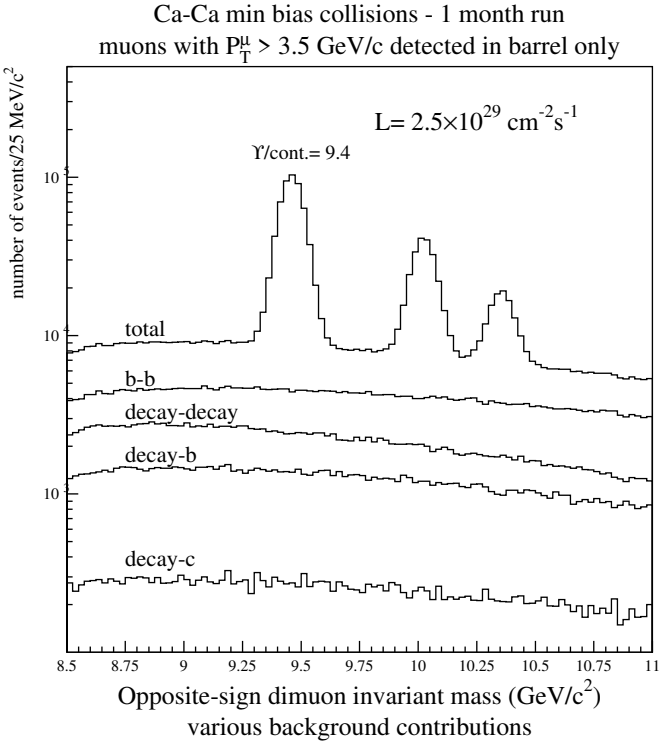

Figure 4: Opposite-sign dimuon mass spectra in the ϒ mass range for Ca-Ca collisions in one month.

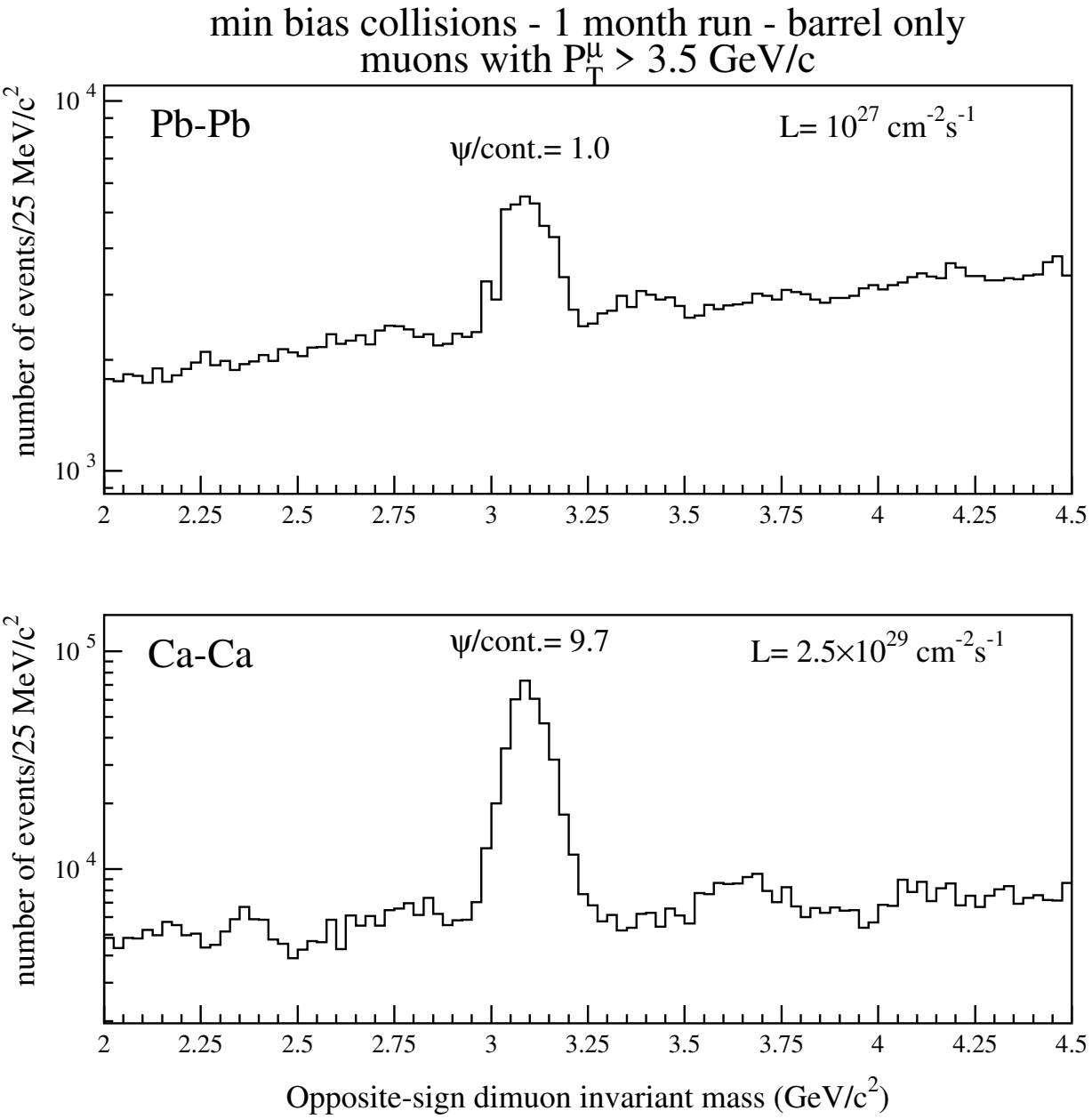

Figure 5: Opposite sign dimuon mass spectra in the J/Ψ mass range for Pb-Pb (up) and Ca-Ca (down) collisions in one month.

5 High mass dimuon production

The distributions of the transverse momentum of muons and the invariant mass of dimuons originating from semileptonic open charm and bottom meson decays are sensitive to the rescattering and energy losses of massive b and c quarks propagating through the dense medium. This process, in combination with high transverse energy jet production (mainly gluon and light quark fragmentation) can give important information about the mechanisms of energy losses of both light and heavy partons in heavy ion collisions. The other process of particular interest is Drell-Yan and Z-bozon production, which are unaffected by final state interactions and can be used as reference process for normalization of heavy quarkonium and hard jet rates in nucleus-nucleus relative to proton-proton collisions.

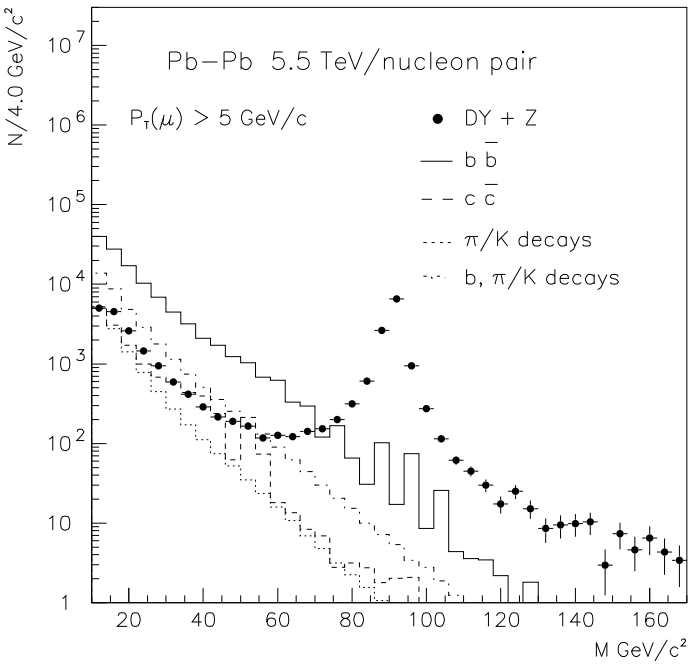

Figure 6: Invariant mass distribution of $\mu^+\mu^-$ pairs for muons with $p_T > 5$ GeV/c in one month of Pb beams.

The main sources of high invariant mass dimuons, with $M > 10$ GeV/c^2 in heavy ion collisions (decays of open heavy flavours ($c\bar{c}$, $b\bar{b}$, $t\bar{t}$), prompt dimuon (Drell-Yan) and Z production, uncorrelated decays of pions and kaons, WW, WZ and ZZ pair production, muon pairs of mixed origin) were investigated in [36]. The heavy flavour, Z, W, WW, WZ and ZZ pair production cross sections in minimum bias AA collisions were extrapolated from those in pp interactions at the same energy ($\sqrt{s} = 5.5$ TeV) using the parameterization $\sigma^i_{AA} = A^2 \times \sigma^i_{pp}$. The corresponding cross section in pp collisions were evaluated using the PYTHIA Monte-Carlo model [34] with default CTEQ2L structure function, and K-factor equal to 2 for $c\bar{c}$ and $b\bar{b}$ production cross section and in the range $1.3 - 1.5$ for Z, W, and $t\bar{t}$ production, taking into account the next-to-leading order pQCD contributions. The dimuon production from uncorrelated hadronic decays has been estimated with the HIJING Monte-Carlo program [29], which gives charged multiplicity density for central and minimum bias $Pb - Pb$ interactions $(dN_{ch}/dy)_{y=0-1} = 8300$ and $(dN_{ch}/dy)_{y=0-1} = 1600$ respectively. The values of dimuon reconstruction efficiencies obtained for various processes in the "central" barrel region $|\eta| < 0.8$ [31] have been taken into account in present simulations.

Figure 6 present opposite sign dimuon invariant mass spectra for muons with $p_T > 5$ GeV/c in one month of Pb beams. A clear signal from $Z \to \mu^+\mu^-$ decays is seen with a background within $M_Z \pm 10$

GeV/c^2 lower than 5%. For two weeks of LHC running time at the luminosity $L = 10^{27}$ cm^{-2}s^{-1}, CMS detector will be able to detect about 11000 events of $Z \to \mu^+\mu^-$ in full rapidity range $|\eta| < 2.4$ with 4300 events in the barrel part of the detector covering $|\eta| < 1.5$. In the mass range 10 GeV/$c^2 \leq M \leq 70$ GeV/c^2 the dominant contribution comes from $b\bar{b}$ fragmentation ($\approx 54\%$). However, while traveling through the dense matter, b quarks may be subject to significant energy losses, which will result in the softening of the muon spectra and suppression of high mass dimuon rates from this source. The mixed origin contribution, when one muon is from $b \to B$ fragmentation and the other from π/K decays is about 16%. The contribution from $c\bar{c}$ fragmentation and π/K decays are 6% and 5% respectively. Note that the uncorrelated part of the background from π/K decays and from mixed origin pairs can be subtracted using like-sign dimuons, as long as the contributions of opposite-sign and like-sign muon pairs are equal. The production rates of dimuons from another sources ($t\bar{t}$, WW, WZ, ZZ) are very low and can be neglected at all available invariant masses.

6 Hard jet pair production

Hard jet production is considered to be an efficient probe for formation of QGP in heavy ion collisions at LHC [37]. However, study of jet characteristics in heavy ion collisions is complicated due to "false" jet background – fluctuations of the transverse energy flow arising from a huge multiplicity of "thermal" secondary particles (up to 8000 charged particles per rapidity unit in a central Pb-Pb collision). Under this condition the reconstruction of "true" QCD jets resulting from hard parton-parton scattering is a vital question. A number of attempts were dedicated to jet finding algorithm optimization in heavy ion collisions under CMS conditions [38, 39, 40].

In order to study the jet recognition for different transverse energy jets in central Pb-Pb collisions with the CMS detector [39], the production cross section of hard jets in minimum bias AA collisions was extrapolated from that in pp interactions at the same energy ($\sqrt{s} = 5.5$ TeV), using the parameterization $\sigma_{AA} = A^2 \times \sigma_{pp}$. The cross-section for QCD jet production in pp collisions was evaluated using the PYTHIA Monte-Carlo program [34], with default structure functions CTEQ2L and a K-factor equal to 1. To estimate the influence of the large number of secondary particles on jet recognition in central Pb-Pb collisions, the high transverse momentum QCD jet events were superimposed on the "thermal" background. The important parameters for this study are: the multiplicity of "thermal" particles (mainly pions and kaons) and their transverse momentum distribution (especially the high p_T tail of the spectra). For the number of charged particles emitted per unit of rapidity in a central $Pb-Pb$ collision (impact parameter $b = 0$), we assume $dN^{\pm}/dy(y = 0) = 8000$, which is the upper limit of most theoretical expectations. Ratios of $N_{\pi^0}/N_{\pi^\pm} = 0.5$ and $N_{K^\pm}/N_{\pi^\pm} = 0.2$ were used independently of the impact parameter. The pseudorapidity distributions of π and K mesons were obtained according to the HIJING event generator [29].

The jet recognition efficiency and expected production rates was studied for the barrel calorimeters $|\eta| \leq 1.5$, detector response being modeled using the CMSJET program [30]. The modified UA1-type jet finding algorithm was used in $\eta - \phi$ space.

Figure 7 presents the sum of the transverse energy depositions in electromagnetic and hadronic calorimeter cells for two high-E_T jets in the central Pb-Pb collision. Although the fluctuations of the transverse energy flow are rather large, jets are still clearly visible over the background. The distributions of the difference in the transverse energy, pseudorapidity and azimuthal angle between the simulated and the reconstructed jets are shown in figure 8, for jets with cone radius $R_{jet} = 0.3$ and transverse energy $E_T \geq 100$ GeV. The precision in the reconstruction of the η and ϕ position of jets is slightly better than for the transverse energy ($\sigma(E_T)/E_T \approx 12\%$, $\sigma(\eta)/R \approx 10\%$ and $\sigma(\phi)/R \approx 6\%$).

Table 3 presents the ratios of reconstructed to simulated jet numbers, relative contribution of "false" jets and transverse energy resolution for jets with different transverse energies. The ratio ϵ_1 of reconstructed to simulated jet numbers is very close to 1. Note that due to the finite jet energy resolution and sharp decreasing the initial dijet spectrum with energy, ϵ_1 can be greater than 1 as well as less. The probability ϵ_2 of "false" jet detection is $12 \pm 3\%$ for $E_T \geq 50$ GeV and becomes negligible for higher transverse energies. The resolution in jet transverse energy improves from 16.7% for $E_T \geq 50$ GeV to 8.6% for $E_T \geq 200$ GeV. For jet transverse energies lower than 50 GeV, the background contribution increases rapidly and the energy resolution is worse.

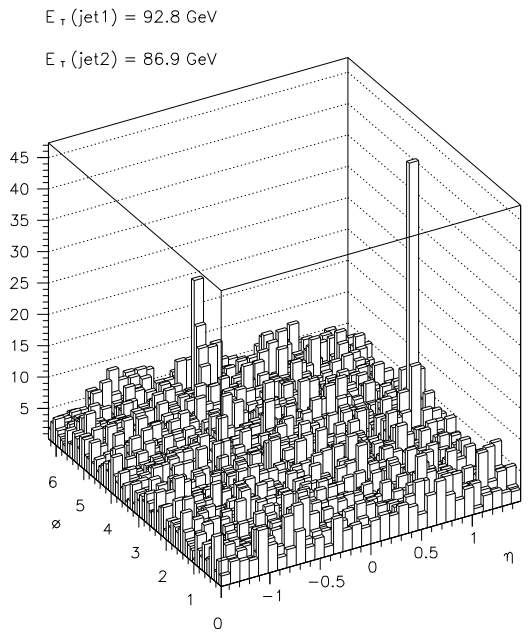

Figure 7: The sum of the transverse energy depositions in electromagnetic and hadron calorimeter cells for high E_T dijet event.

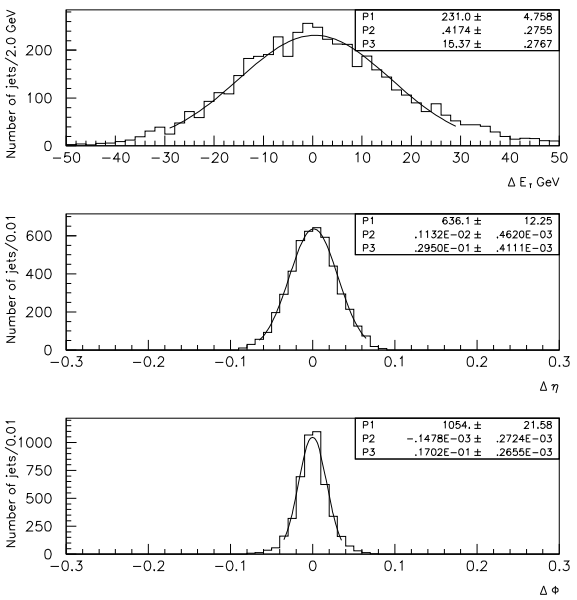

Figure 8: Distributions of differences in transverse energy, pseudorapidity and azimuthal angle between the simulated and reconstructed jets (P_1, P_2 and P_3 are the constant, mean and σ parameters of Gaussian fit respectively). $R_{jet} = 0.3$ and $E_T^{jet} \geq 100$ GeV.

Table 3: Ratio of reconstructed to simulated jet numbers ϵ_1, contribution of "false" jets ϵ_2 and transverse energy resolution for jets with different transverse energies

$E_T \geq$, GeV	ϵ_1	ϵ_2	$\sigma(E_T)/E_T$, %
50	0.94 ± 0.03	0.120 ± 0.030	16.7
100	1.03 ± 0.02	0.010 ± 0.004	11.6
150	0.98 ± 0.02	0.004 ± 0.003	9.2
200	0.99 ± 0.02	0.004 ± 0.003	8.6

The internal structure of jets has been also investigated in [38, 40]. In this case the CMS calorimeter response was modeled using the CMSIM-008 version adopted for heavy ions collisions and shower parameterization for hadron calorimeter in the pseudorapidity range $\mid \eta \mid < 3$. It has been found two criteria, which allow the optimization of jet finding algorithms to be made using a different intrinsic structure of "false" and "true" hard QCD-jets.

1. Rms radius of a jet can be introduced as $< R >= \sum_i R_i \cdot (E_i - \overline{E_T})/E_T^{jet}$, where R_i is the distance between cell i covered by the jet and the center of the jet in the $\eta - \phi$ space, E_{Ti} and E_T^{jet} are the transverse energy (minus background $\overline{E_T}$) of the cell and the jet respectively. Figure 9a presents the rms radius of "false" jet (as calculated with "thermal" model) and "true" hard jet of $R_{jet} = 0.5$ (calculated with PYTHIA [34] model) versus jet energy E_T^{jet} (without energy losses of hard jet). The selection criterion $< R > /R_{jet} < 0.5$ allows the major part ($\approx 95\%$ at $E_T^{jet} > 100$ GeV) of the "false" background jets to be removed, the signal being almost not sensitive ($< 5\%$) to this cut.

2. The energy density in center region of a jet can be introduced as a ratio of the sum of transverse energy of cells covered by the jet within radius $r = 0.7R_{jet}$ to the total jet energy. Figure 9b shows the energy density of "false" jet and "true" hard jet of $R_{jet} = 0.5$ versus jet energy E_T^{jet}. We can see that the selection criterion $E_T\ (r < 0.7R_{jet})/E_T^{jet} > 0.7$ allows the bulk of the "false" jets to be removed again.

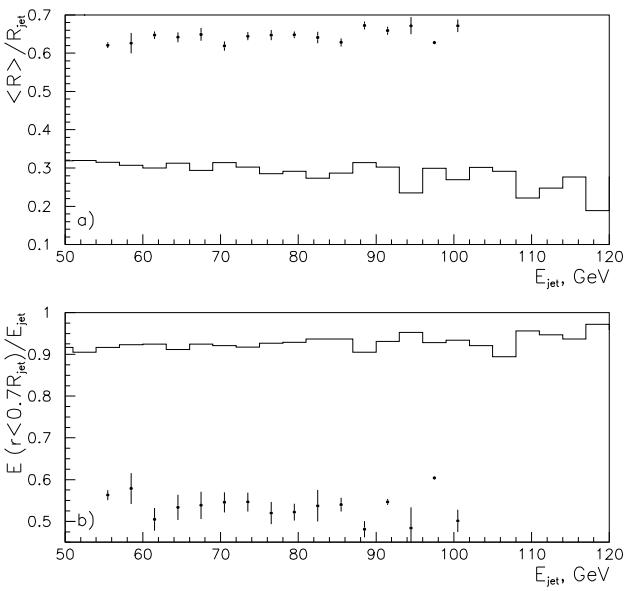

Figure 9: Rms radius $< R >$ (a) and the transverse energy density $E_T\ (r < 0.7R_{jet})/E_T^{jet}$ (b) of "true" hard jet (histogram) and "false" jet (points) versus jet energy E_T^{jet}, $R_{jet} = 0.5$.

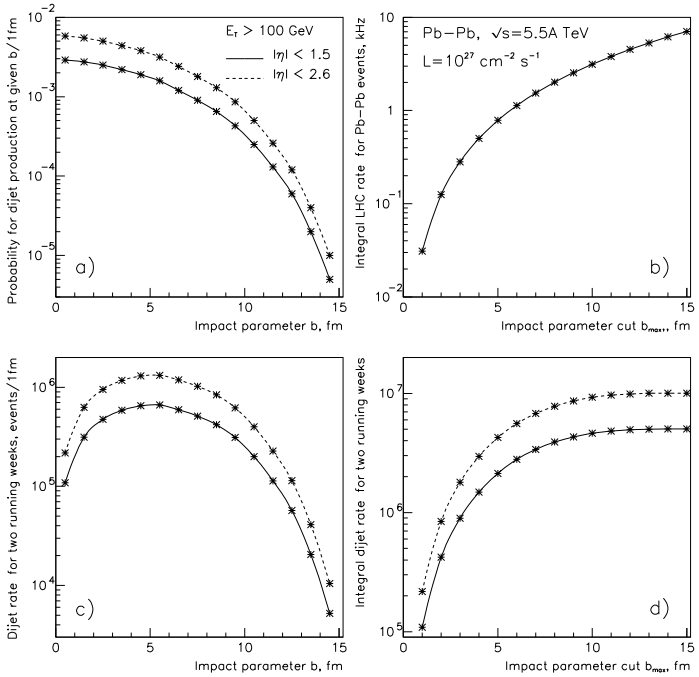

Figure 10: Data for dijet production ($E_T^{jet} > 100$ GeV, $\mid \eta \mid < 1.5$ and $\mid \eta \mid < 2.6$) in Pb-Pb collisions as a function of the impact parameter b. (a) – differential probability of dijet production at given b, (b) – integral LHC rate for Pb-Pb collisions at luminosity $L = 10^{27} cm^{-2} sec^{-1}$, (c) and (d) – the differential and integral rates of initially produced dijets for two weeks LHC running time.

The dependence of jet pair production rates on impact parameter of Pb-Pb collisions has been studied in [37] assuming the model of independent inelastic nucleon-nucleon sub-collisions. The cross section of hard process is a strongly increasing function of centrality of collisions (see figure 10a for differential probability of dijet production with $E_T^{jet} > 100$ GeV for different CMS acceptance, $\mid \eta \mid < 1.5$ and $\mid \eta \mid < 2.6$). Figure 10b represents integral LHC rate for Pb-Pb collisions assuming luminosity $L \simeq 1 \times 10^{27}\ cm^{-2} s^{-1}$. The total rate of inelastic Pb-Pb interactions is about 8 kHz, but one can see, for example, that we have only 2.5% events ($\approx$ 200 Hz rate) with $b < 2.5$ fm. The differential and integral dijet rates for 1 month of Pb beams with half of the time devoted for data taking (1.3×10^6 s) as a function of the impact parameter are presented in figures 10c and 10d respectively. The total rate of dijets with $E_T^{jet} > 100$ GeV is 1.1×10^7 events for $\mid \eta \mid < 2.6$, and it reduces by factor ~ 2 if only barrel part of CMS calorimeters $\mid \eta \mid < 1.5$ is considered. The collisions with impact parameter $b < 6$ fm contribute $\approx 50\%$ in total dijet rates, only 15% dijets being produced in the collisions with $b < 2.5$ fm. If the luminosity has to be shared between two experiments, the luminosity for each experiment will be about one fourth of the design one. Even in this case the expected statistics will be large enough to study the dijet rates as a function of impact parameter b.

In order to test the sensitivity of the final hadronic jet characteristics to the energy losses [40], three different scenarios for jet quenching due to collisional energy losses of jet partons were studied [18]: (i) no jet quenching, (ii) jet quenching in a perfect quark-gluon plasma (the average collisional losses of a hard gluon $< \Delta E_g > \simeq 9$ GeV, $< \Delta E_q > = 4/9 \cdot < \Delta E_g >$), (iii) jet quenching in a maximally viscous quark-gluon fluid, resulting in $< \Delta E_g > \simeq 18$ GeV. The initial conditions for a gluon dominated plasma ($N_f \sim 0$) formation in central Pb-Pb collisions at LHC energies were used as estimated in [19] using the new HERA parton distributions: the proper time of the QGP formation $\tau_0 \sim 0.1$ fm/c, the initial QGP temperature $T_0 \sim 1 GeV$. The "hard" central Pb-Pb collision is generated as the superposition of "thermal" event and one hard PYTHIA pp-event. The response of the barrel part of CMS calorimeters

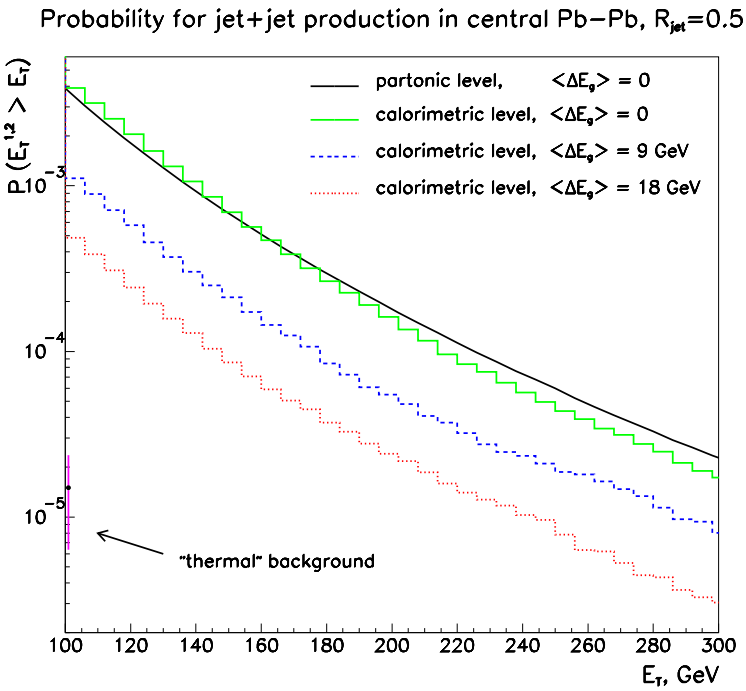

Figure 11: The probability of dijet yield with transverse energy $E_T^{jet1,2} > E_T$ in central Pb-Pb collisions for different jet quenching scenarios: "true" hard (histograms) and "false" (point) dijets, $dN^{\pm}/dy(y=0) = 8000$. The additional criterion on rms radius of a jet $< R > /R_{jet} < 0.5$ being used ($R_{jet} = 0.5$). Solid curve shows the scaled result ($\propto$ number of inelastic nucleon-nucleon sub-collisions) for dijet spectrum at partonic level as calculated with PYTHIA model.

has been modeled with the fast simulation model [40]. Figure 11 represents the probability of dijet yield as a function of the energy detection threshold E_T, the rms radius criterion of a jet $< R > /R_{jet} < 0.5$ ($R_{jet} = 0.5$) being used. The significant suppression of hard dijet yield due to energy losses (up to factor ~ 7, or somewhat higher if the radiative energy losses mechanism is included) can be expected. One can see that the quenching factor being almost independent of the jet energy if the losses do not depend (or even depend weakly) on the energy of an initial hard parton.

7 $Z(\rightarrow \mu^+\mu^-) + jet$ and $\gamma + jet$ production

The dominant channels for high transverse momentum $Z + jet$ and $\gamma + jet$ production are $q + g \rightarrow q + Z$ and $q + g \rightarrow q + \gamma$ respectively. Thus the bulk of detected jets going to be quark-induced in such processes. Contrary to the gluon-dominated dijet production where one could investigate jet quenching due to mostly gluon energy losses in dense matter, $Z + jet$ and $\gamma + jet$ processes give a possibility to study quark energy losses. The jet energy losses should result in the non-symmetric shape of the distribution of differences in P_T between the Z-boson (γ) and jet. Note that we are not measuring energy losses of a leading quark by such way, but getting total losses of quark-initiated jet outside the given jet cone.

The estimated statistics is rather low for $Z(\rightarrow \mu^+\mu^-) + jet$ channel: about 900 events with $P_T^{Z,\ jet} > 50$ GeV/c in the pseudorapidity range $|\ \eta\ | < 3.0$ produced in Pb-Pb collisions for two weeks LHC running time, the background being less than 10% in this case [37]. However because of much higher luminosity for lighter ions the expected statistics for Ca-Ca collisions is 12000 $Z(\rightarrow \mu^+\mu^-) + jet$ events for the same period of running time even for 10 times less luminosity than the design one.

On the other hand, using $\gamma + jet$ production is complicated due to large background from $jet + jet$ production when one of the jet in an event is misidentified as a photon (the leading π^0): the estimated number of events with $E_T^{jet,\gamma} > 100$ GeV produced in Pb-Pb collisions for two weeks LHC running time are 7800 signal events and 1.1×10^7 background events [41, 37]. However, the shape of the distribution

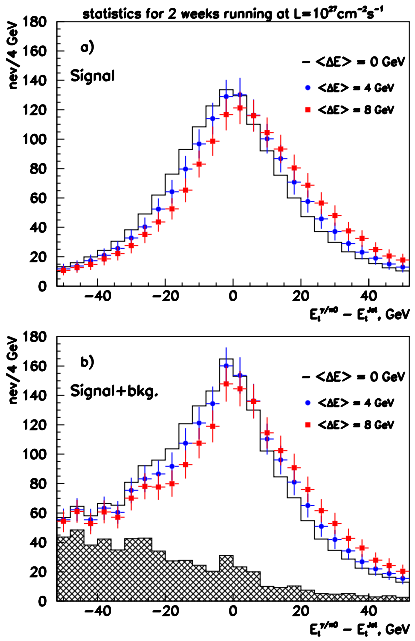

Figure 12: The distributions of differences in transverse energy between the γ and jet with $E_T^{\gamma,\ jet} > 120$ GeV for two weeks running time (a) without (π^0 + jet) background counting, b) with (π^0 + jet) background counting) in the rapidity region $\mid y^{\gamma,\ jet} \mid < 1.5$ for different values of jet energy losses (initial state gluon radiation and finite jet energy resolution are taken into account).

of differences in transverse energy between the γ and jet is very different for signal and background, and still sensitive to the jet quenching effect. Figure 12 shows the distributions of differences in transverse energy between the γ and jet with $E_T^{\gamma,\ jet} > 120$ GeV for two weeks LHC running time (without and with $(\pi^0 + jet)$ background counting) in the rapidity region $\mid y^{\gamma,\ jet} \mid < 1.5$ for different values of jet energy losses, the modified photon trigger algorithm being used [41]. We expect about 1600 signal and 2200 background events in this case. For the region of $(E_T^{\gamma} - E_T^{jet}) > 0$ there is a difference for almost every bin grater than 1 standard deviation for the rather small jet energy losses 8 GeV and even for the losses 4 GeV. It seems possible to subtract the background $\pi^0 + jet$ events from the experimental spectra using the background shape from Monte-Carlo simulation and (or) from pp data.

8 Conclusion

To summarize, we have considered the capability of the CMS detector for heavy ion physics at Large Hadron Collider. A good muon system and electromagnetic and hadron calorimeters with fine granularity gives the possibility to cover several important aspects of the heavy ion physics. Since the detector is optimized for the accurate measurement of the characteristics of high-energy muons, photons, electrons, and hadron jets, it going to be useful for studying hard probes of the quark-gluon plasma in heavy ion collisions. In particular, the production of heavy quarkonia Υ, Υ', Υ'' through their muon decay channel and the energy losses of hard quark- and gluon-initiated jets, are valuable processes for studying the earliest stages of heavy ion collision evolution.

Despite the huge multiplicity of secondary particles, the reconstruction of the Υ resonances from their decay dimuons is feasible with a 66% efficiency in the worst case, corresponding to a central Pb-Pb collisions with 8000 charged particles per rapidity unit. The total number of Υ events reconstructed in one month of Pb-Pb data taking amounts to 22000 and the signal-to-background ratio is 1.6 in the Υ mass region in the most pessimistic case.

The resolution in jet transverse energy has been found from 16.7% at $E_T \geq 50$ GeV for the barrel part

of CMS calorimeters, decreasing to 8.6% for $E_T \geq 200$ GeV. Using the selection criterion on jet internal structure allows getting the maximum efficiency of "true" hard jets recognition as well as the maximum suppression of "false" jet background. The expected statistics for dijet production will be large enough to study dijet rates as a function of impact parameter of the collision and the transverse energy of jets. The suppression of dijet rates (jet quenching) due to energy losses of hard partons expected to be much more stronger at very central collisions in comparison with the peripheral one's.

Other possible signatures that could directly observe the energy losses involve tagging the hard jet opposite a particle that does not interact strongly ($\gamma + jet$ and $Z(\rightarrow \mu^+\mu^-) + jet$ channels). The jet energy losses should result in the non-symmetric shape of the distribution of differences in transverse momentum between the Z-boson (γ) and jet. The estimated statistics is rather low for $Z(\rightarrow \mu^+\mu^-)$ + jet channel. On the other hand, using $\gamma + jet$ production is complicated due to large background from $jet+jet$ production when one of the jet in an event is misidentified as a photon (the leading π^0). However the shape of the distribution of differences in transverse energy between the γ and jet is very different for signal and background, and still sensitive to the jet energy losses.

The main contribution to high invariant mass ($M > 10$ GeV/c^2) opposite-sign dimuon spectra in heavy ion collisions comes from semileptonic open bottom meson decays and prompt dimuon (Drell-Yan) and Z production. The significant energy losses of massive b quarks traveling through the dense matter should result in the observed softening of the muon spectra and suppression of high mass dimuon rates. This process, in combination with high transverse energy jet production (mainly gluon and light quark fragmentation) can give important information about the mechanisms of energy losses of both light and heavy partons in heavy ion collisions. $Z(\rightarrow \mu^+\mu^-)$ production will be detected in heavy ion collisions with a small background ($< 5\%$), and can be used as reference process for normalization of heavy quarkonium and hard jet rates in nucleus-nucleus relative to proton-proton collisions.

Transverse energy deposition in barrel, end-cap and very forward parts of the CMS calorimeters strongly depends on the impact parameter of nucleus-nucleus collision, This will allow one to measure the centrality of the collisions and to study the dependence of the characteristics of hard production processes (heavy quarkonia, high mass dimuons, $jet + jet$, $\gamma + jet$ and $Z + jet$ channels) on the impact parameter, in the whole range from peripheral to central collisions.

Finally, Monte-Carlo study shows that CMS detector is well suited for the investigation of dimuons and high transverse energy jets, production of which are important for extracting information about the properties of super-dense matter to be created in heavy ion collisions at LHC.

References

[1] H.Satz. Phys. Rep. 88 (1982) 349

[2] I.L.Rozental', Yu.A.Tarasov. Usp. Fiz. Nauk 163 (1993) 29

[3] I.M.Dremin, A.V.Leonidov. Usp. Fiz. Nauk. 165 (1995) 759

[4] J.W.Harris , B.Muller Annual Rev. of Nucl. and Part. Science 46 (1996) 71

[5] I.P.Lokhtin, L.I.Sarycheva, A.M.Snigirev. Phys. Part. Nucl. 30 (1999) 279

[6] J.Engels et al. Phys. Lett. 396 B (1997) 210; E.Laermann. Phys. Part. Nucl. 30 (1999) 304

[7] Proc. of Quark-Matter'96, Nucl. Phys. A (610) 1996; Proc. of Quark-Matter'97, Nucl.Phys. A 638 (1997)

[8] T.Matsui, H.Satz. Phys. Lett. 178 B (1986) 416

[9] D.Kharzeev , H.Satz. Phys. Lett. 334 B (1994) 155

[10] M.Gonin et al. (NA50 Coll.) Nucl. Phys. A 610 (1996) 404

[11] J.-P.Blaizot, J.-Y.Ollitrault. Rev. Lett. 77 (1996) 1703; C.-Y.Wong. Phys. Rev. C 55 (1997) 2621; D.Kharzeev, M.Nardi, H.Satz. Phys. Lett. 405 B (1997) 14

[12] S.Gavin, R.Vogt Phys. Rev. Lett. 78 (1997) 1006; A.Capella, A.Kaidalov, A.Kouider Akil, C.Gerschel. Phys. Lett. 393 B (1997) 431

[13] M.G.Ryskin. Sov. J. Nucl. Phys. 52 (1990) 139

[14] M.Gyulassy, X.-N.Wang. Nucl. Phys. B420 (1994) 583; X.-N.Wang, M.Gyulassy, M.Plumer. Phys. Rev. D51 (1995) 3436

[15] R.Baier, Yu. L.Dokshitzer, S.Peigne, D.Schiff. Phys. Lett B 345 (1995) 277; R.Baier, Yu. L.Dokshitzer, A.H.Mueller, S.Peigne, D.Schiff. Nucl. Phys. B 483 (1997) 291; 484 (1997) 265; R.Baier, Yu. L.Dokshitzer, A.H.Mueller, D.Schiff. Nucl. Phys. B 531 (1998) 403; Phys. Rev. C58 (1998) 1706

[16] B.G.Zakharov. JETP Lett. 65 (1997) 615

[17] S.Mrowczynski. Phys. Lett. B 269 (1991) 383; M.H.Thoma. Phys. Lett. B 273 (1991) 128

[18] I.P.Lokhtin, A.M.Snigirev. Phys. At. Nucl. 60 (1997) 360; Z.Phys C73 (1997) 315

[19] K.J.Eskola, K.Kajantie, P.V.Ruuskanen, Phys. Let. B 332 (1994) 191

[20] I.P.Lokhtin, A.M.Snigirev. Phys. Lett. B 440 (1998) 163

[21] M.Gyulassy, M.Plumer. Phys. Lett. B 234 (1990) 432

[22] M.Plumer, M.Gyulassy, X.-N.,Wang. Nucl. Phys. A590 (1995) 511

[23] V.Kartvelishvili, R.Kvatadze, R.Shanidze. Phys. Lett. B 356 (1995) 589

[24] X.-N.Wang, Z.Huang, I.Sarcevic. Phys. Rev. Lett. 231 (1996) 77

[25] E.Shuryak. Phys. Rev. C 55 (1997) 961; Z.Lin, R.Vogt, X.-N.Wang. Phys. Rev. C57 (1998) 899

[26] CMS Collaboration, Technical Proposal, CERN/LHCC 94-38

[27] M.V.Savina, S.V.Shmatov, N.V.Slavin, P.I.Zarubin. JINR Rapid Communications 1 (1998) 45

[28] V.Kartvelishvili, R.Kvatadze. CERN CMS NOTE 1999/015

[29] X.-N.Wang, M.Gyulassy. Phys. Rev. D 44 (1991) 3501; Comput. Phys. Commun. 8 (1994) 307

[30] S.Abdullin, A.Khanov, N.Stepanov. CERN CMS TN 1994/180

[31] M.Bedjidian, O.Kodolova. CERN CMS NOTE 1999/004

[32] M.Bedjidian, O.Drapier. CERN CMS NOTE 1999/052

[33] F.Abe et al. (CDF Collab.). Phys. Rev. Lett. 75 (1995) 4358

[34] T.Sjostrand. Comput. Phys. Commun. 82 (1994) 74

[35] C.Charlot et al. CERN CMS TN 1993/063

[36] M.Bedjidian, V.Kartvelishvili, R.Kvatadze. CERN CMS NOTE 1999/017

[37] I.P.Lokhtin et al. CERN CMS NOTE 1999/016

[38] N.A.Kruglov, I.P.Lokhtin, L.I.Sarycheva, A.M.Snigirev. Z. Phys. C 76 (1997) 99

[39] M.Bedjidian, R.Kvatadze, V.Kartvelishvili. CERN CMS NOTE 1997/082

[40] I.P.Lokhtin, L.I.Sarycheva, A.M.Snigirev, I.N.Vardanyan. CERN CMS NOTE 1998/025

[41] A.Nikitenko et al. CERN CMS NOTE 1998/063